Biogeotechnics 4 (2026) 100188

Contents lists available at ScienceDirect

Biogeotechnics

journal homepage: www.keaipublishing.com/en/journals/biogeotechnics/

3D printing and lab-scale testing of bio-inspired geogrids for road rutting reduction

Jiaojun Liu[a,*], Nimisha Roy[b], J. David Frost[c]

[a] College of Civil Engineering, Tongji University, Shanghai 200092, China
[b] School of Computing Instruction, Georgia Institute of Technology, Atlanta, GA 30332, USA
[c] School of Civil and Environmental Engineering, Georgia Institute of Technology, Atlanta, GA 30332, USA

ARTICLE INFO

Keywords:
Geogrids
Spider webs
Bio-inspired design
Rutting

ABSTRACT

The utilization of geogrids to mitigate road rutting, or permanent deformation, has significantly increased over the last decade. However, faced with ever-increasing traffic loads, commonly used commercially available biaxial and triaxial geogrids cannot always provide an optimal solution. There is an urgent need for developing the next generation of geogrids that will be more cost-effective and outperform current options. This paper utilizes 3D printing technology to fabricate geogrids inspired by spider webs, and evaluates their relative performance using a lab-scale testing system. The testing apparatus comprises a miniature road structure with two layers: a top base course layer made of aggregates and a bottom subgrade layer made of locally sourced soil. A wheel moves cyclically to simulate traffic loads. Additionally, the testing program incorporates 3D scanning at various stages using a handheld scanner to digitize changes to critical surfaces, such as the top of the road and the interface between the base course and the subgrade. These digitized data are used to compare the relative performance of different geogrids. The lab-scale testing results reveal that, although the new bio-inspired geogrid did not show significant additional improvement in reducing surface rutting for the lab-scale road, the bio-inspired geogrid helped distribute traffic load to a larger area of the subgrade than some existing commercial products.

Introduction

Road rutting, also known as permanent surface deformation, is typically caused by repeated vehicle loads along the wheel path. Road rutting can lead to passenger discomfort, traffic accidents, and expensive road repairs. With ever-increasing traffic volumes, roads that last longer and minimize rutting development are highly desirable. One effective solution to the road rutting issue is the incorporation of geogrids in the pavement system. Geogrids are human-made polymer grid structures designed to address unfavorable soil conditions. Previous geogrid studies (Douglas, 1997; Haas et al., 1988; Halliday & Potter, 1984) have shown that, when utilized for road applications, geogrids can reduce road rutting, extend the road's service life, and lower construction and maintenance costs.

Geogrids have been used in road construction since the early 1980s. The most common geogrid geometries are square/rectangular (biaxial) and triangular (triaxial). However, advancements in manufacturing techniques, such as 3D printing, can allow for the creation of innovative geogrid structures, prompting manufacturers to develop new geometries that enhance rutting performance. As the quality of available soil worsens and high-quality base course aggregates become scarce, along with the increased use of recycled construction materials, many existing geogrid designs are becoming less effective. This has led to growing interest in advanced geogrids that offer improved performance and adapt better to challenging site conditions.

However, most current geogrid applications still focus on these traditional, readily available geogrids. This study aims to address this gap by designing and evaluating novel geogrid geometries to guide the development of the next generation of geogrids. This research has two primary goals: to scientifically design new geogrid geometries and to evaluate their performance in the lab.

Bio-inspired geogrid design

To scientifically design new geogrid geometries, the bio-inspired design method was chosen. Bio-Inspired Design (BID), or biomimicry, is a method that imitates or draws inspiration from nature's forms and processes to solve human problems (Benyus, 2009). In recent years, BID

* Corresponding author.
E-mail address: liujiaojun@tongji.edu.cn (J. Liu).

https://doi.org/10.1016/j.bgtech.2025.100188
Received 22 April 2025; Received in revised form 29 May 2025; Accepted 13 June 2025
Available online 20 June 2025
2949-9291/© 2026 The Authors. Publishing services by Elsevier B.V. on behalf of KeAi Communications Co. Ltd. This is an open access article under the CC BY license (http://creativecommons.org/licenses/by/4.0/).

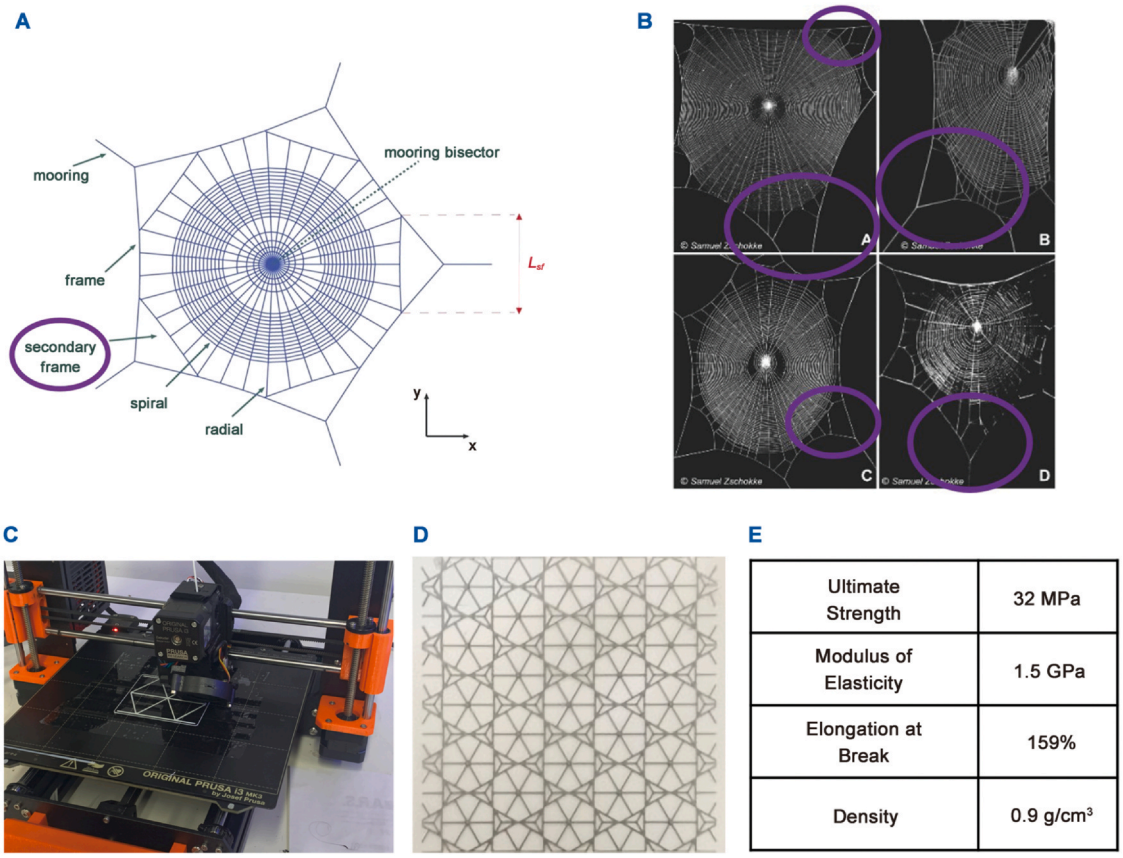
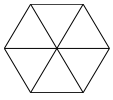
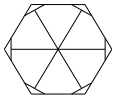
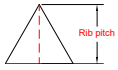


Fig. 1. (**A**) Simplified spider web model with secondary frame; (**B**) Examples of orb webs with secondary frames (right) (Soler & Zaera, 2016); (**C**) Prusa i3 3D printer; (**D**) 8" by 8" geogrid testing samples; (**E**) Polypropylene filament properties.

Table 1

Geogrid	Unit Cell	# of secondary ribs per unit cell	Rib pitch, $\frac{\sqrt{3}}{2}l$, mm (in.)	Rib depth, *t*, mm (in.)	Rib width, *b*, mm (in.)
Tri		0	20.32 (0.80)	1.27 (0.05)	1.016 (0.04)
Y_L		6			

has been applied to geotechnical engineering (Martinez, 2022). For example, BID has been used to address geotechnical engineering challenges such as subsurface burrowing (earthworm-inspired burrowing machines (Borela et al., 2021; Zhang et al., 2024)), soil and rock penetration (angelwing clam-inspired boring machines (Zhao & Dai, 2023)), anisotropic soil-structure interface shear (snake-skin-inspired directional piles (O'Hara and Martinez, 2022)), and slope or foundation anchorage (root-inspired ground anchors (Mallett et al., 2021)).

In this research, the spider web serves as the primary source of bio-inspiration for new geogrid designs. Previous studies (Craig, 1987a, 1987b) have shown that some spider web structures are carefully designed to absorb more impact energy than a single silk (thread). For example, the energy-absorbing capabilities of whole webs built by *Micrathena schreiberi* are about an order of magnitude higher than the energy-absorbing properties of the web's frame silks and two orders of magnitude higher than the energy-absorbing properties of the web's viscid silks.

Soler and Zaera (2016) found that the superior energy absorption in some 2D Orb Weaver webs is related to specific structural features. For instance, certain spider webs have secondary frames, or "Y" structures, positioned between the radial and outer frame threads (as shown in Fig. 1A and B). These structures prevent the radial threads from connecting directly to the outer frame's corners (anchors). The role of the secondary frame is to distribute impact loads more effectively across the entire web, preventing load concentration and increasing the web's energy-absorbing capacity.

Inspired by spider web's secondary frame ("Y" structure), this research devises Geogrid Y_L, a spider web-inspired geogrid. Table 1 compares the traditional triaxial geogrid (Tri) with the Y_L geogrid; both have the same rib pitch, depth, and width, but the Y_L includes secondary frames.

Bio-inspired geogrid prototyping

Polypropylene (PP) geogrid samples, each measuring 0.2 m (8 in.) by 0.2 m (8 in.), were 3D-printed using an Original Prusa i3 printer (Fig. 1C). The printed structure is shown in Fig. 1D and some PP filament properties are listed in Fig. 1E.

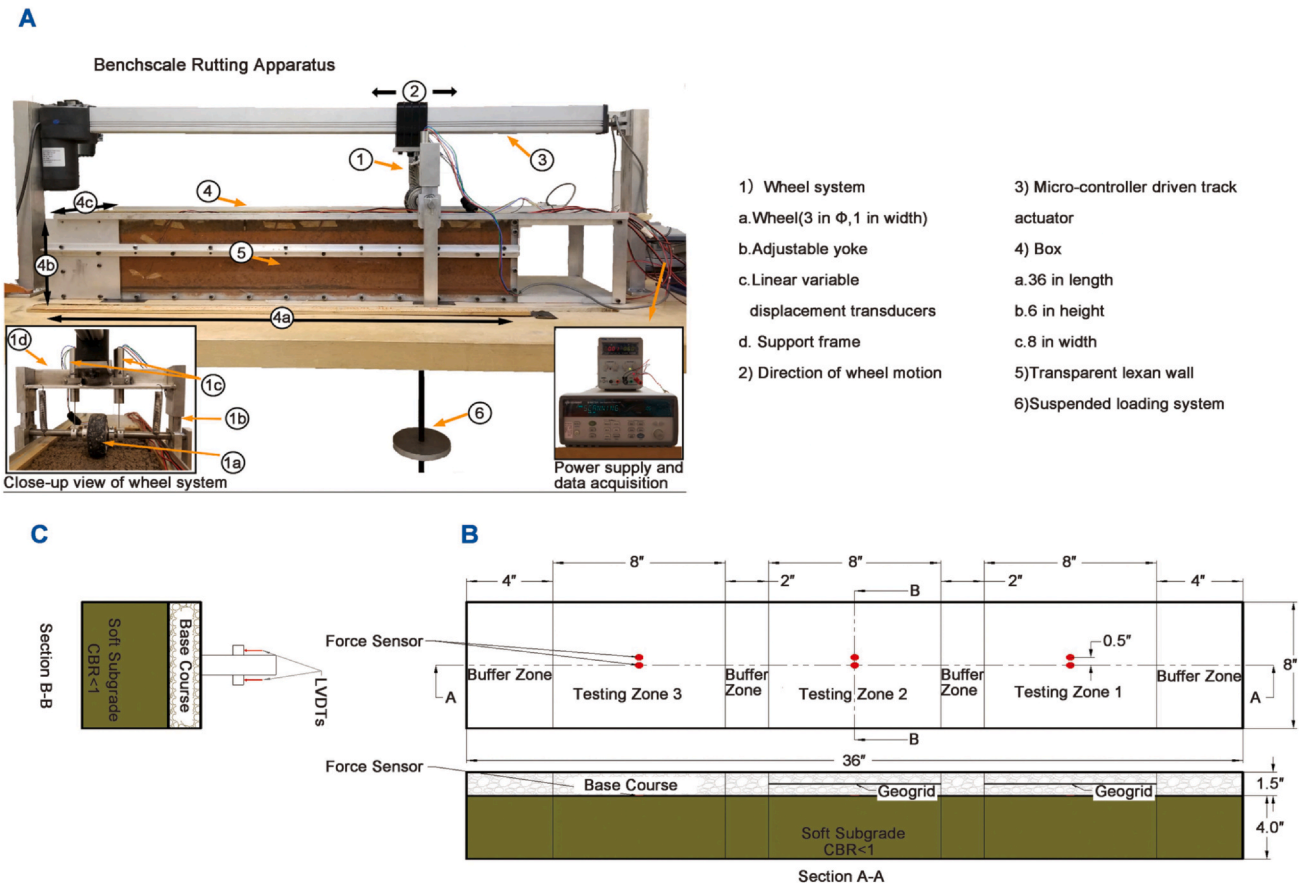


Fig. 2. (**A**) Bench scale rutting test apparatus (Hanumasagar, 2019); (**B**) Plan view (top) and profile view (bottom) of the bench test section. Force sensors (red dots) were installed at the base course–subgrade interface, two per test zone (one directly under the wheel path and one 0.5 in beside the wheel path). (**C**) Side view of lab-scale road with LVDTs mounted on both sides of the wheel (indicated by the red arrows).

Table 2
Subgrade soil properties (left) and aggregate properties (right).

Subgrade soil		Base course aggregate	
	Red Georgia Soil		Angular rock
USCS Classification	SC	USCS Classification	GP
Percentage Fines (%)	12.7	Average particle size (D50) (mm)	5.5
Plastic Limit (%)	31		
Liquid Limit (%)	40	e_{max}	0.94
PI (%)	8	e_{min}	0.78
Max. Dry Density (pcf)	95		
Optimal Water Content (%)	26		

Bio-inspired geogrid rutting performance testing

To assess the effectiveness of newly prototyped geogrids in reducing road rutting, bench-scale rutting tests were conducted. These tests assessed the performance of lab-scale two-layer pavement sections (test roads) consisting of an aggregate base course over a subgrade soil.

The test equipment is shown in Fig. 2A and comprised of the following components:

- Testing box: A steel containment box measuring 0.91 m (36 in) in length, 0.2 m (8 in) in width, and 0.15 m (6 in) in depth was used to construct the pavement sections (test roads).
- Cyclic traffic load simulation system: A wheel with a diameter of 0.089 m (3.5 in) and a width of 0.032 m (1.25 in) was mounted on a linear actuator to simulate repeated traffic loading. The wheel traveled at a speed of 0.47 in/s. Additional loading was applied using a dead-load suspension system to achieve a tire contact pressure of 475 kPa (68.86 psi). The wheel's motion was precisely controlled by an Arduino-based PID controller.
- Data acquisition system: Data from all instruments was collected at a frequency of 2 Hz by the data acquisition system.

The test layout is shown in Fig. 2B. Each bench-scale test section (test road) contained three individual test zones, which could either be unreinforced control zones or geogrid-reinforced test zones, with each zone reinforced by a different prototyped geogrid. Each test zone measured 0.2 m (8 in) in width and 0.2 m (8 in) in length. The test zones consisted of a nominal 4-inch-thick subgrade (though, after compaction, the actual thickness of the subgrade layer was less than 4 in) placed in four lifts. Additionally, the test zones were surfaced with a 1.5 in thick base course, placed in one lift, mimicking typical construction practices over extremely soft subgrades.

The lab-scale road material and instrumentation are discussed below.

Materials

The subgrade soil for the lab-scale road is locally sourced red Georgia soil. The soil properties are summarized in Table 2.

The target water content for the subgrade is 28.5 % (wet of optimum) to create a weak subgrade that can lead to road rutting due to subgrade bearing capacity failure, and the California Bearing Ratio (CBR) at the targeted moisture content is 0.76 % ($CBR_{0.2\ in} = 0.76\%$). Typically, if the subgrade soil's CBR value is less than 2 %, subgrade replacement or improvement is necessary. Therefore, all lab-scale roads constructed for this study have poor subgrade conditions.

The base course for the lab-scale road consisted of angular, uniformly sized crushed aggregate. Aggregate properties are also presented in Table 2, and the aggregates are compacted to a dry density of 1607.33 kg/m^3.

To use these materials to construct lab scale road, the subgrade was constructed in four lifts. After the subgrade was installed and levelled, a layer of loose aggregate was spread over it. A geogrid was then laid on top of this supportive aggregate layer, followed by another confining aggregate layer placed over the geogrid. Both aggregate layers were compacted together in one lift to mobilize base-geogrid interlocking and to compact the base course effectively.

Instrumentations

The following instruments were used to monitor the deformation and load of the test zones:

- Force sensor (also called load cell in this research):
  Vertical stresses were measured using the FlexiForce A201 Sensor, with two sensors installed per test zone. The location of the force sensors is detailed Fig. 2B. This arrangement facilitated the measurement of stress distributions at the base course-subgrade interface.
- Linear Velocity Displacement Transducer (LVDT):
  Road surface vertical deflections were monitored using a Trans-Tek Model 0245–00000 linear velocity displacement transducer (LVDT). The layout of LVDTs is shown in Fig. 2C.
- 3D Scanner:
  An EinScan Pro HD Handheld 3D Scanner (accuracy up to 0.004 in) was employed for 3D scanning to digitize crucial surfaces both before and after traffic load cycles, facilitating detailed analysis of surface deflection. Table 3 illustrates an example of the digitalized top surface of the road (top of the base course) and the interface between the base course and subgrade. Table 3 also showcases an example of an average cross-section, where the green portion represents the range of all surface cross-sections in the test zone, while the red line signifies the generated average surface. Fig. 3A presents a sample cross-section from the scans and Fig. 3B explains how the rutting was quantified. Here:
- Densification rutting is defined as the maximum vertical downward displacement due to cyclic loading.
- Total rutting includes both densification and upward shear deformations, measured as the difference between the peak and valley of the rut profile.

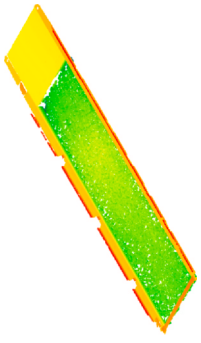
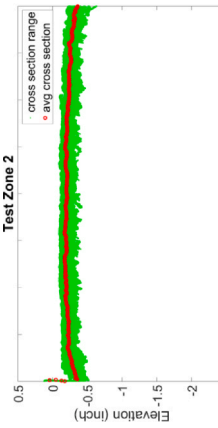
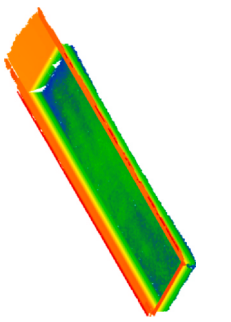
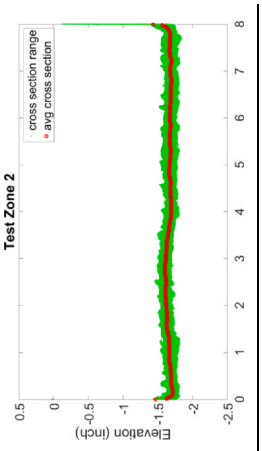
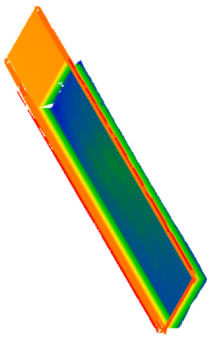
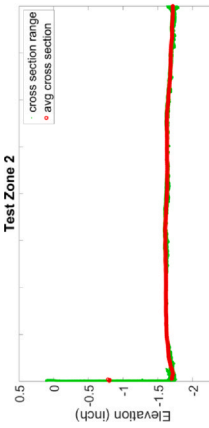
Fig. 3C illustrates the average cross-section for the Tr80 (triaxial) geogrid–reinforced test zone, from which both total and densification rutting are measured.

In summary, two instruments were utilized to measure surface deformations: LVDTs monitored the development of deformation at the top of the road with increasing traffic cycles, while 3D scanners aided in assessing the overall permanent deformation for both the top of the road and the base course-subgrade interface before and after completion of the test. Additionally, force sensors, which may also be referred to as load cells in this study, were employed to evaluate traffic load distribution on the base course-subgrade interface.

Rutting test results

The surface rutting development data monitored by the LVDTs is shown in Fig. 4A. The LVDT data indicate that Tr80 (purple line in Fig. 4A) and Y80_L (red line in Fig. 4A) follow similar rutting trends,

Table 3
Surfaces digitalization and cross section generation.

	Before cyclic load		After cyclic load	
	3D scanned data	Example of average surface's cross section generated	3D scanned data	Example of average surface's cross section generated
Top of road				
Base course – subgrade interface				

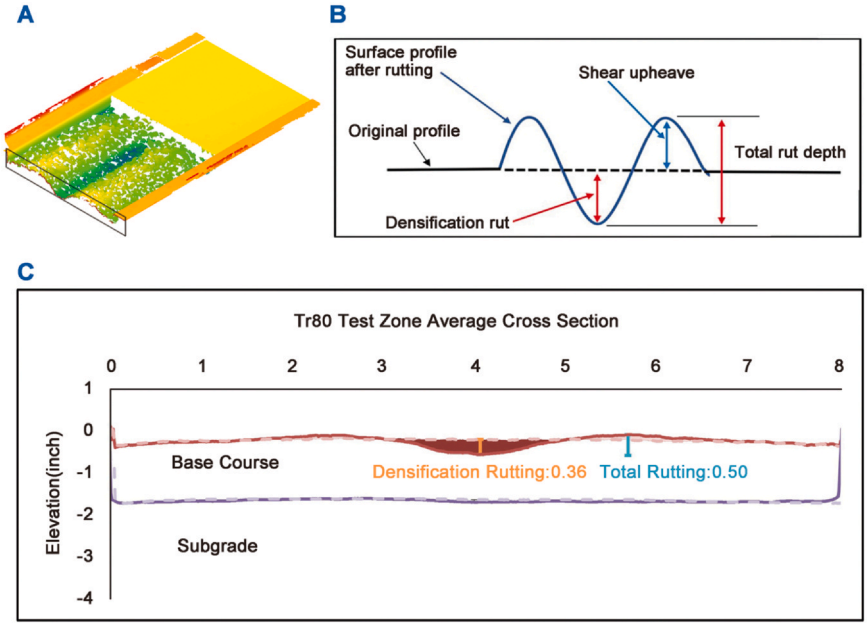


Fig. 3. Information derived from the 3D scanned data: (**A**) Example cross-section from the 3D scan; (**B**) Quantitative measurements of rutting based on the cross-section. Densification rutting refers specifically to the maximum vertical displacement before and after loading. Notably, the deformation captured by LVDTs at the road surface primarily reflects densification. Total rutting includes both densification and shear deformation and is measured as the difference between the peak and valley of the rut profile (Shaheen et al., 2017). (**C**) Average cross-section of the Tr80 (triaxial) geogrid-reinforced test zone and corresponding rutting measurements (total rutting and densification rutting).

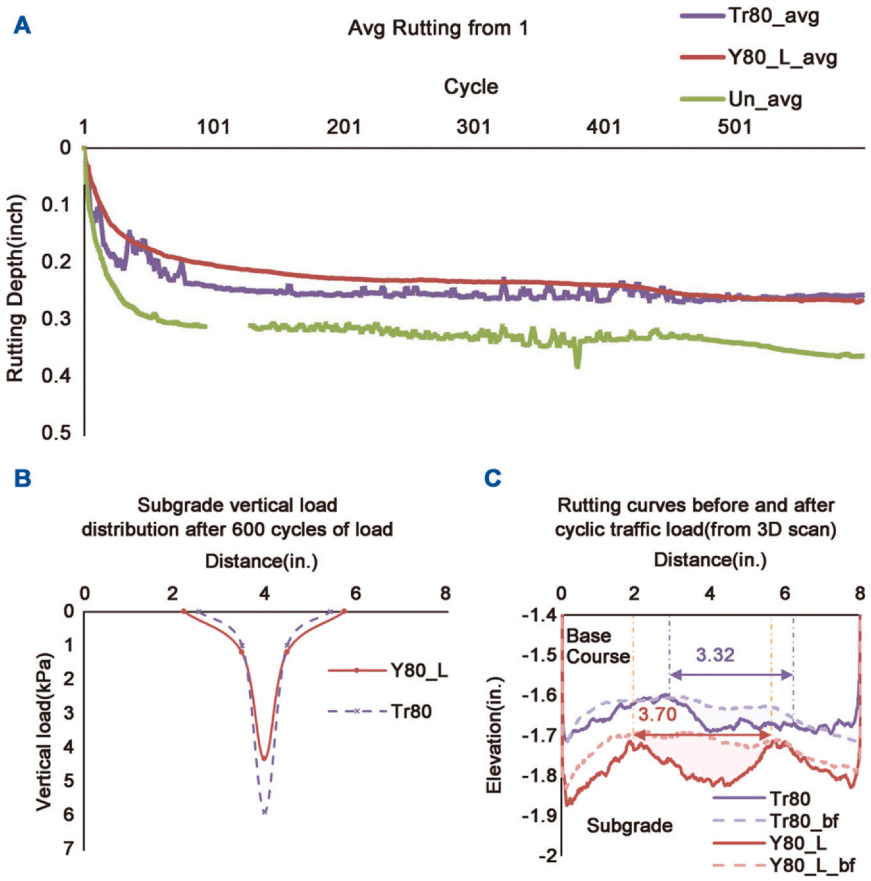


Fig. 4. (**A**) Surface Deformation Development for Test Zones - Unreinforced (Un), Triaxial Geogrid Reinforced (Tr80), and Y Geogrid with Secondary Frame Reinforced (Y80_L); (**B**) Vertical stress distribution at 600 traffic load cycles; (**C**) Interface deformation before and after cyclic traffic load for Tr80 and Y80_L reinforced test zones.

Table 4

Geogrid	Total rutting (in.)	Densification rutting (in.)
Un	0.62	0.43
Tr80	0.50	0.36
Y80_L	0.47	0.32

with both reinforced zones exhibiting less rutting than the unreinforced test zone (green line in Fig. 4A).

The 3D scanned data is summarized in Table 4. The 3D scanned data also indicates that Tr80 and Y80_L show similar rutting depths that are smaller than those of the unreinforced test zone. Both Tr80 and Y80_L reduce total surface rutting and densification rutting by approximately 20 %.

The similarity in rutting depths for Tr80 and Y80_L may result from the lab-scale two-layer road's subgrade having a very low CBR (less than 1 %), indicating a weak subgrade. Under cyclic traffic loading, the Y80_L reinforced test zone may experience a slightly lower vertical load on the subgrade than the Tr80 reinforced zone; however, even for Y80_L reinforced test zone, this vertical load still likely exceeds the subgrade's bearing capacity. Consequently, both reinforced zones undergo significant subgrade deformation, masking any differences in rutting behavior between the two geogrids. Further laboratory tests using stronger subgrades are recommended to better distinguish the rutting performance of the traditional triaxial geogrid (Tr80) versus the Y geogrid (Y80_L).

Although the traditional triaxial geogrid (Tr80) and Y geogrid (Y80_L) did not show a significant difference in rutting performance for the lab-scale road (based on LVDT and 3D scan data), the load cell data indicate that the Y geogrid (Y80_L) provides a less concentrated vertical stress distribution over a wider area compared to the traditional triaxial geogrid (Tr80) (Fig. 4B).

The 3D scanned data of the base course – subgrade interface also show that the Y geogrid helps distribute traffic load to a wider area on subgrade by about 10 % (increasing from 3.32 in to 3.70 in, as shown in Fig. 4C).

Conclusions

Previous studies on spider webs have suggested that secondary frames, or "Y" structures, can help distribute load over a larger area and increase the web's energy-absorbing capacity. In this research, a bio-inspired geogrid with a Y structure was designed and prototyped. The performance of the new geogrid on a lab-scale two-layer road was tested. Bench-scale rutting test results indicate that, although the new bio-inspired geogrid did not show significant improvement in surface rutting for the lab-scale two-layer road, the load cell data indicate that the Y geogrid helps distribute traffic load to a larger area on the subgrade.

The key intellectual contributions of this study include:

- The use of 3D printing allowed for the production of lab-scale geogrid samples with new geometries, expanding the research scope beyond traditional manufacturing methods.
- 3D scanning technology replaced labor-intensive single profile tools like straight-edges and rulers for surface deformation analysis, providing detailed data before and after deformation and enabling a comprehensive analysis of rutting behavior.

Overall, the study combines lab-scale cyclic loading tests with innovative technologies to provide new insights into geogrid rutting reduction performance.

Future work

To build on these findings, the following future research directions are proposed:

- Perform tests with stronger-subgrade materials
  Repeat bench-scale rutting tests on stiffer subgrades (CBR $\geq$ 5 %) to prevent large subgrade bearing-capacity failure from masking geogrid effects.
- Use alternative 3D-printing materials
  Fabricate and test geogrids using various filaments—PLA, PET-G, TPU, and fiber-reinforced—to vary geogrid material tensile strength and ductility. Combining different polymer properties with novel geogrid geometries will reveal how material–geometry synergies influence rutting performance.
- Explore synergistic material–geometry optimization

Previous research shows that triaxial geogrids perform better than biaxial geogrids for road rutting reduction (Abu-Farsakh & Chen, 2011; Abu-Farsakh et al., 2012; Sharbaf & Ghafoori, 2021) and extensible PP geogrids outperform inextensible steel geogrid for road rutting reduction (Hanumasagar, 2019). However, when looking at nature webs (2D Orb-Weaving Spider Webs), previous biological studies have shown that spider webs owe their superior performance not just to the properties of the web material, but also from its alignment within the geometry of the web (McKeag, 2014). This indicates that the web material and web geometry work together to generate superior performance—what can be termed the synergetic effect between web material and geometry. Future work should leverage these biomechanical insights to systematically explore which material–geometry combinations maximize load distribution and rutting resistance.

CRediT authorship contribution statement

Jiaojun Liu: Writing – original draft, Methodology, Investigation, Formal analysis, Data curation. **Nimisha Roy:** Writing – review & editing. **James David Frost:** Writing – review & editing, Supervision, Project administration, Funding acquisition, Conceptualization.

Declaration of Competing Interest

The authors declare that they have no known competing financial interests or personal relationships that could have appeared to influence the work reported in this paper.

Acknowledgements

The findings presented in this manuscript are based on work supported in part by the US National Science Foundation through PTE Federal Award No. EEC-1449501. Any opinions, findings and conclusions or recommendations expressed in this material are those of the authors and do not necessarily reflect the views of the National Science Foundation. Additional funding was provided by the Chinese Scholarship Council and the Elizabeth and Bill Higginbotham Professorship in the School of Civil and Environmental Engineering at Georgia Tech.

References

Abu-Farsakh, M. Y., & Chen, Q. (2011). Evaluation of geogrid base reinforcement in flexible pavement using cyclic plate load testing. *International Journal of Pavement Engineering, 12*(3), 275–288. https://doi.org/10.1080/10298436.2010.549565

Abu-Farsakh, M. Y., Souci, G., Voyiadjis, G. Z., & Chen, Q. (2012). Evaluation of factors affecting the performance of geogrid-reinforced granular base material using repeated load triaxial tests. *Journal of Materials in Civil Engineering, 24*(1), 72–83. https://doi.org/10.1061/(asce)mt.1943-5533.0000349

Benyus, J. M. (2009). *Biomimicry: Innovation inspired by nature.* New York, NY: Harper Collins.

Borela, R., Frost, J. D., Viggiani, G., & Anselmucci, F. (2021). Earthworm-inspired robotic locomotion in sand: An experimental study with X-ray tomography. *Géotechnique Letters, 11*(1), 66–73. https://doi.org/10.1680/jgele.20.00085

Craig, C. L. (1987a). The significance of spider size to the diversification of spider-web architectures and spider reproductive modes. *The American Naturalist.* https://doi.org/10.1086/284622

Craig, C. L. (1987b). The ecological and evolutionary interdependence between web architecture and web silk spun by orb web weaving spiders. *Biological Journal of the Linnean Society, 30*(2), 135–162. https://doi.org/10.1111/j.1095-8312.1987.tb00294.x

Douglas, R. A. (1997). Repeated-load behaviour of geosynthetic-built unbound roads. *Canadian Geotechnical Journal, 34*(2), 197–203. https://doi.org/10.1139/cgj-34-2-197

Haas, R., Walls, J., & Carroll, R. G. (1988). Geogrid reinforcement of granular bases in flexible pavements. *Transportation Research Record, 1188*(1), 19–27.

Halliday, A.R., & Potter, J.F. (1984). The performance of a flexible pavement constructed on a strong fabric, *TRRL Laboratory Report*, 1123.

Hanumasagar, S. S. (2019). *Experimental and computational evaluation of geomaterial interactions in flexible pavementsDoctoral dissertation*Georgia Institute of Technology.

Mallett, S. D., Frost, J. D., & Huntoon, J. A. (2021). Root-inspired anchorage systems for uplift and lateral force resistance. *IFCEE, 2021*, 299–307. https://doi.org/10.1061/9780784483411.029

Martinez, A., Dejong, J., Akin, I., Aleali, A., Arson, C., Atkinson, J., et al. (2022). Bio-inspired geotechnical engineering: Principles, current work, opportunities and challenges. *Géotechnique, 72*(8), 687–705. https://doi.org/10.1680/jgeot.20.P.170

McKeag, T. (2014). Little things multiply up: Hierarchical structures. *Zygote Quarterly, 9*, 10–27.

O'Hara, K. B., & Martinez, A. (2022). Load transfer directionality of snakeskin-inspired piles during installation and pullout in sands. *Journal of Geotechnical and Geoenvironmental Engineering, 148*(12), 04022110. https://doi.org/10.1061/(ASCE)GT.1943-5606.0002929

Shaheen, M., Al-Mayah, A., & Tighe, S. (2017). Effects of high friction aggregate and PG Plus binder on rutting resistance of hot mix asphalt mixtures. *International Journal of Pavement Engineering, 18*(4), 292–302. https://doi.org/10.1080/10298436.2015.1065996

Sharbaf, M., & Ghafoori, N. (2021). Laboratory evaluation of geogrid-reinforced flexible pavements. *Transportation Engineering, 4*, Article 100070. https://doi.org/10.1016/j.treng.2021.100070

Soler, A., & Zaera, R. (2016). The secondary frame in spider orb webs: The detail that makes the difference. *Scientific Reports, 6*(1), https://doi.org/10.1038/srep31265

Zhang, W., Huang, R., Xiang, J., & Zhang, N. (2024). Recent advances in bio-inspired geotechnics: From burrowing strategy to underground structures. *Gondwana Research, 130*, 1–17. https://doi.org/10.1016/j.gr.2023.12.018

Zhao, Y., & Dai, S. (2023). Challenges of rock drilling and opportunities from bio-boring. *Biogeotechnics, 1*(1), Article 100009. https://doi.org/10.1016/j.bgtech.2023.100009